Theoretical analysis of anomalous conductivity in Hall Effect Thrusters

IEPC-2005-21

Presented at the 29th International Electric Propulsion Conference, Princeton University October 31 – November 4, 2005

A. Ducrocq*, J.C. Adam†, A.Héron‡and G. Laval§

Centre de Physique Théorique, Ecole Polytechnique, CNRS UMR 7644,Palaiseau, 91128, France

Numerous evidences exist today that the classical conductivity cannot explain the behavior of Hall Thrusters. Numerical models have also shown that wall collisions are insufficient to provide enough conductivity. On the other hand, with the help of an implicit particle code, we have shown that the parameter range of interest, the plasma inside the thruster is turbulent and that this turbulence is sufficient to reproduce its behavior. In this paper, we present a linear study of the electron drift instability that we have identified in the implicit model. We solve numerically the dispersion relation for various parameters. One of the conclusions is that the wave vector of the instability is essentially perpendicular to the magnetic field. We will pay attention to the drift modes. We have developed an explicit 2D PIC code to study the nonlilear behavior of the preceding instability. This model confirms the linear growth rate computed theoretically and also shows without ambiguity that the developement of electrostatic perturbations is associated with the flow of current even in the presence of a single mode. In single mode case, we have built a simple theoretical model similar to the one used for heating of Tokamaks by electromagnetic waves. This model shows that at sufficiently large amplitude of the electrosatic field, stochasticity is induced in the gyromotion of the electrons.

*Ph.D. student, Ecole Polytechnique, Alexandre.Ducrocq@cpht.polytechnique.fr
†Directeur de Recherche, CNRS, Jean-Claude.Adam@cpht.polytechnique.fr
‡Chargé de Recherche, CNRS, heron@cpht.polytechnique.fr
§Professeur émérite , CNRS, laval@cpht.polytechnique.fr

I. Introduction

The experiments on the SPT-100ML thruster (Stationary Plasma Thruster), the numerical simulations[1,2−7] and more recently the works on the lower power cylindrical Hall Thruster[8] show that the contribution of the classical electron-atom collisions to cross-field transport is insignificant. On the other hand, plasma turbulence[9−11] seems more and more involved in the process of anomalous transport even though the way it occurs still remains unknown. Thus, J.C. Adam and A. Heron have developed a fully kinetic two-dimensional model of the Hall thruster in order to study the stability of the plasma in the direction of rotation due to the $E \times B$ drift [1]. They have demonstrated that the large drift velocity that inherently exists at the exhaust of the thruster can be responsible for an instability that gives rise to plasma turbulence. This instability is a high frequency one with very short wave length. The study of this kinetic instability has a real interest insofar as a wave with high wavenumber is more efficient in term of diffusion. This present paper is devoted to the derivation and to the study of the dispersion relation of electrostatic waves in a hot magnetized electron beam drifting across a magnetic field with non magnetized cold ions. We demonstrate that the simplified description of the plasma configuration of Hall Thrusters, i.e. the uniform cross-field configuration only, is enough to generate unstable waves of frequencies ω as $\Omega_{ci} \ll \omega \ll \Omega_{ce}$, where Ω_{ci}, Ω_{ce} are respectively the ion and electron gyro frequencies with high wave numbers. This leads to an instability connected to the resonance between kV_d, where k is the wave number and V_d the drift velocity, and the cyclotron harmonics $n\Omega_{ce}$ where n is an integer. The properties found thanks to this study will be used to build a theoretical model descibing the interaction of the instability with the electrons in the thruster. We will see that this model provide a better understanding of the origin of the anomalous transport. The plan of this work is as follows: Section II is devoted to the linear study of the electron drift instability. The dispersion relation is established, focusing on the drift modes. We pay attention on the influence of the temperature and of the density gradient on the instability. In the Section III,we will exposed the theoretical model for electron transport and its results. To conclued, section **??**, we will show several results from the PIC simulations which highlight the strong correlation between the evolution of the electrostatic energy and the mean velocity across the magnetic field.

II. Linear study of the electron drift instability

A. Derivation of the dispersion relation

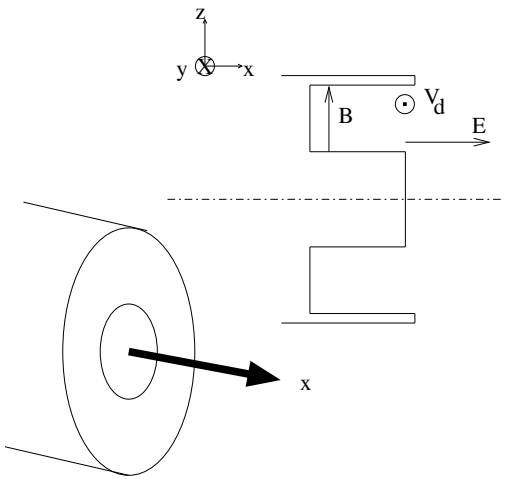

Figure 1. Schema of the geometry used for the calculation.

The plasma configuration we consider here is the Hall Thruster one. As shown in Fig.1, a magnetic field is applicated to the plasma in the radial direction which will be the z direction and an electric field is created in the x longitudinal direction. This cross-field configuration drives an electron current with velocity V_d in the azimuthal direction which stands for y in all the following. We assume that the ions are not affected by the electric and magnetic fields on the time scale we look at. It leads to ignore the ion drift in our equilibrium, retaining only that of the electrons. It can be done insofar as we only consider the case $\gamma \gg \Omega_{ci}$ where γ is a typical growth rate for the instabilities to be discussed. Several studies[12−14] of unstable waves have already been performed in such plasma configurations, but they usually take into account a magnetic field gradient or a density gradient. Here, we neglect them both assuming that the stationary electric field drift velocity V_d is much larger than the magnetic field gradient drift velocity and than the density gradient drift velocity. This assumption restricts the following stability analysis to wavelengths far below the magnetic field and density gradient lengths. However, we will see that the wavelengths of the unstable modes are close to the Larmor radius or even smaller. So we can argue that the magnetic field gradient is insignificant indeed. As for the density gradient, a brief study of his influence will be done further. Thus, for the unperturbed plasma, we have :

$$\vec{E} = E_0 \ \vec{e_x} \tag{1}$$

$$\vec{B} = B_0 \ \vec{e_z} \tag{2}$$

$$n(x,y,z) = n_0 \ ; \ \vec{V_d} = -\tfrac{E_0}{B_0}\vec{e_y} \tag{3}$$

We study the behavior of a pure electrostatic perturbation. The perturbed potential is written: $\Phi = \Phi_0 \ exp[i(k_x x + k_y y + k_z z - \omega t)]$ where k_x, k_y, k_z are the components of the wave number vector. The ions are considered as cold so we describe them in a simple way by a cold fluid. Then, the equations of the hydrodynamic we take for the ions are:

$$M(\tfrac{\partial}{\partial t} + \vec{v_i}.\vec{\nabla}).\vec{v_i} = -e\vec{\nabla}\Phi \tag{4}$$

$$\tfrac{\partial n_i}{\partial t} + \vec{\nabla}.n_i\vec{v_i} = 0, \tag{5}$$

where n_i and v_i are the ion density and velocity, e is the ion charge and M is the ion mass.

Linearizing and resolving the system in order to find the perturbed density of ion, we obtain:

$$n_i^1 = \frac{n_0 e\Phi k^2}{M\omega^2} \tag{6}$$

where $k^2 = k_x^2 + k_y^2 + k_z^2$.

The electrons at the equilibrium are described by a classical Maxwellian distribution function with a temperature T, shifted by the velocity V_d in the direction y:

$$f_0 = n_0\Big(\frac{m}{2\pi T}\Big)exp\Big[-\frac{v^2 - V_d^2}{2v_{th}^2}\Big] \tag{7}$$

where $v_{th} = \sqrt{\frac{T}{m}}$ is the thermal velocity, m is the electron mass.

Taking into account the perturbation, the electron distribution function f_e satisfies the Vlasov equation:

$$\frac{\partial f_e}{\partial t} + \vec{v_e}.\frac{\partial f_e}{\partial \vec{r}} - \frac{e}{m}\Big[-\vec{\nabla}\Phi + \vec{v_e} \times \vec{B}\Big].\frac{\partial f_e}{\partial \vec{v_e}} = 0 \tag{8}$$

where v_e is the electron velocity vector.

We linearize the function f_e and integrate the Vlasov equation resulting along the unperturbed orbits in the well known way [15]. We find the perturbed density of electrons:

$$n_e^1 = \frac{e}{m}\frac{n_0\Phi}{v_{th}^2}\Big\{1+\xi\Big\{Z(\xi)I_0(b)e^{-b}+\sum_{n=1}^{n=\infty} I_n(b)e^{-b}(Z(\xi+\frac{n\Omega}{k_z v_{th}\sqrt{2}})+Z(\xi-\frac{n\Omega}{k_z v_{th}\sqrt{2}}))\Big\}\Big\} \quad (9)$$

where $\xi = \frac{\omega - k_y V_d}{k_z v_{th}\sqrt{2}}$ and $b = \frac{k_\perp^2 v_{th}^2}{\Omega^2}$ with $k_\perp^2 = k_x^2 + k_y^2$. The functions I_n are modified Bessel functions of order n. Z is the plasma dispersion function of Fried & Conte [14]: $Z(\eta) = \frac{1}{\sqrt{\pi}}\int_{-\infty}^{\infty}\frac{e^{-t^2}}{t-\eta}dt$

The set of equations (6) and (9), and the Poisson's equation determine the dispersion relation:

$$k^2\lambda_D^2\Big(1-\frac{m}{M}\frac{\omega_{pe}^2}{\omega^2}\Big) + 1+\xi\Big\{Z(\xi)I_0(b)e^{-b}+\sum_{n=1}^{n=\infty} I_n(b)e^{-b}(Z(\xi+\frac{n\Omega}{k_z v_{th}\sqrt{2}})+Z(\xi-\frac{n\Omega}{k_z v_{th}\sqrt{2}}))\Big\} = 0 \quad (10)$$

where $\lambda_D^2 = \frac{T}{m\omega_{pe}^2}$ is the Debye length, ω_{pe} being the electron plasma frequency.

The full study of the three dimensional dispersion relation (10) to be published[15] conlued that the wave vector of the instability is essentially perpendicular to the magnetic field. In the next part, we will pay attention to the drift modes only. We will also go back over the assumption of homogeneous density by introducing a gradient in the longitudinal direction x.

B. Drift modes equation, $k_x = k_z = 0$

We obtain the drift modes by assuming $k_x = k_z = 0$. The Z function yields:

$Z(\eta) \approx -\eta^{-1}(1+\frac{1}{2\eta^2})$

And the dispersion relation becomes:

$$k_y^2\lambda_D^2\Big(1-\frac{m}{M}\frac{\omega_{pe}^2}{\omega^2}\Big)+\Big[1-I_0(b)e^{-b}+\sum_{n=1}^{n=\infty}\frac{2(\omega-k_y v_d)^2 I_n(b)e^{-b}}{(n\Omega)^2-(\omega-k_y v_d)^2}\Big] = 0 \quad (11)$$

with $b = \frac{k_y^2 v_{th}^2}{\Omega^2}$

We introduce the density gradient by linearizing the density profile about the density of reference n_0. The density is written now as $n = n_0(1+x/L_n)$ where L_n is the gradient length defined by $\frac{1}{L_n} = \frac{1}{n_0}\frac{dn}{dx}$. It yields the dispersion relation:

$$k_y^2\lambda_D^2\Big(1-\frac{\omega_{pi}^2}{\omega^2}(1+\frac{x}{L_n})\Big) =$$

$$\Big(1+\frac{x}{L_n}\Big)\Big\{I_0(b)e^{-b}-1+\sum_{n=1}^{n=\infty}\frac{2(\omega-k_y v_d)^2 I_n(b)e^{-b}}{(\omega-k_y v_d)^2-(n\Omega)^2}\Big\}+\frac{k_y v_{th}^2}{\Omega L_n}\Big\{\sum_{n=1}^{n=\infty} I_n(b)e^{-b}\frac{2(\omega-k_y V_d)}{(\omega-k_y V_d)^2-(n\Omega)^2}+\frac{I_0(b)e^{-b}}{\omega-k_y V_d}\Big\} \quad (12)$$

where ω_{pi0}, ω_{pe0} are the ion and electron plasma frequencies at the origin ($x = 0, n = n_0$).

Considering a cold plasma, $b \ll 1$, it reduces to:

$$\Big(1-\frac{\omega_{pi0}^2}{\omega^2}\Big) = \omega_{pe0}^2\Big(\frac{1}{(\omega-k_y V_d)^2-\Omega^2}+\frac{1}{\Omega k_y L_n(\omega-k_y V_d)}\Big) \quad (13)$$

We solve the equation and we obtain waves almost purely growing with a rate given by:

$$\omega_i = \omega_{pi0}(1-\beta)\sqrt{\frac{(kV_d)^2-\Omega^2}{\omega_{UH}^2-(kV_d)^2}} \quad (14)$$

with $\beta = \frac{\omega_{pe0}^2((k_y V_d)^2-\Omega^2)}{2\Omega k_y L_n k_y V_d((k_y V_d)^2-\omega_{UH}^2)}$

The roots are unstable for $\Omega < kV_d < \omega_{UH}$ where $\omega_{UH}^2 = \omega_{pe0}^2 + \Omega^2$ is the upper hybrid resonant frequency. For $b \ll 1$, the value of the growth rate depends on L_n but the existence of the unstable modes do not. So we find the result already determined for the Hall thrusters in the homogeneous case in REF.[1]: for $V_d/v_{th} < 1$, no more unstable roots are found with $b \ll 1$. Back to the more general case of a hot plasma, we notice that the introduction of the gradient density in the calculation of the dispersion relation brings a new term in relation to the Eq. (11) with the coefficient proportional to: $\frac{1}{k_y L_n \Omega} = \frac{1}{k_y V_d}\frac{V_d}{v_{th}}\frac{r_L}{L_n}$ where r_L is the Larmor radius. In plasmas of interest for Hall thrusters, the drift velocity is close to the thermal velocity and the parameter $k_y V_d$ is high compare to the unit. So, the gradient length has to be largely smaller than the Larmor radius so that the additional term in Eq. (12) would be significant. Thus, the density gradient will probably not change the results until it reaches a value largely higher than the ones existing in the Hall thrusters.These results are displayed on the next figures which show numerical solutions of the dispersion relations established in this part.

C. Numerical results

In the temporal theory of instability, the perturbations are expanded into instability waves $exp[-i(\omega t - \vec{k}.\vec{r})]$, the wave numbers k are real, and the complex frequency $\omega = \omega_r + i\omega_i$ must be a solution respectively to Eq.(11), (12). The unstable modes correspond to positive growth rates ω_i. For the sake of simplicity, dimensionless variables will be used in the following. The quantities ω, Ω and k will denote ω/ω_{pe}, Ω/ω_{pe} and kV_d/ω_{pe}, respectively. The thermal velocity will normalise the drift velocity. The dispersion relation has been solved using these new parameters. We assume the cyclotron frequency as $\Omega/\omega_{pe} = 0.1$. In the framework of Hall thruster, it amounts to a magnetic field of 170 G for a density of 2.8 10^{11} particles per cm^3. Taking the drift velocity equal to $V_d = 2\ 10^6 m.s^{-1}$, these paramaters correspond to the values mesured in the simulations [1] at the location where the instability developped, in the case of a discharge voltage of 300V. The following results have been calculated for the mass ratio of xenon $m/M = 4.2\ 10^{-6}$ which is the propellant used most of the time in Hall thruster.

1. *Unstable modes*

We have solved Eq.(11) numerically to find the dependence of ω_r and ω_i on wave number k_y. Figure 2 shows the frequency of the unstable modes and the corresponding growth rate as a function of the wave number in the azimuthal direction k_y for a fixed ratio $V_{th}/V_d = 0.5$. We can see the transitions from stability to instability whenever $k_y V_d$ is close to a cyclotron harmonic $n\Omega$. The growth rate reaches a maximum and then decreases sharply between each cyclotron harmonic. Each growth rate peaks are separated by stable regions. The real part of the solutions is plotted in logarythmic units in Fig.2 so that one could see that the frequency is several orders of magnitude below the growth rate except in the vicinity of the growth rate peak. Figure 2(a) is a zoom on the small wave number of the figure 2(b).

Figure 2(b) represents the envelop of the frequency and of the growth rate as a function of $k_y V_d$ from small to very large wave numbers. The values of ω_r correspond to frequencies ranging from $1MHz$ to $50MHz$ which agrees with the range of frequencies observed in the PIC simulations [1]. These frequencies are associated with very large values of growth rate which corresponds to growth times ranging from $0.1\mu s$ down to $0.01\mu s$. The envelop has a maximum value for $k_y V_d/\omega_{pe}$ around 1.2. Thus, maximum of the growth rate is reached for wave length close to the tenth of a millimetre. The unstable modes spread over a very great range of wave number. For a wave number approaching $4.10^4 m^{-1}(k_y V_d/\omega_{pe} = 10)$, the growth rate is still significant as his value is the quarter of the one of the growth rate peak.

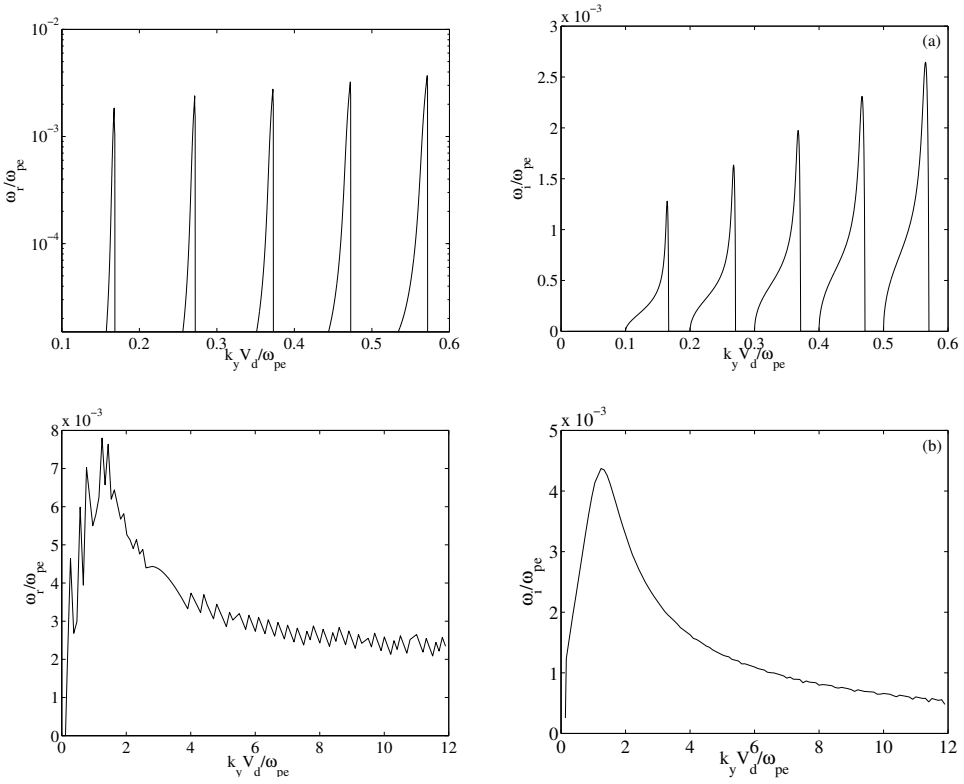

Figure 2. Numerical solutions of the one dimensional dispersion relation. (a) represents the real part and the imaginary part as a function of $k_y V_d$. (b) is the corresponding envelop from small to very large wave numbers. The cyclotron frequency is equal to 0.1 in dimensionless value.

2. Evolution of the unstable modes as a function of thermal velocity

In order to discuss our choice of thermal velocity in the resolution of the dispersion relation Eq.(11), the growth rate ω_i is shown in Fig.3 as a function of V_{th}/V_d and of $k_y V_d$. The unstable modes still exists for high temperature as great value of the growth rate can be observed, even for values of V_{th}/V_d as large as 2. Nevertheless, the width of the stable regions increases with the increase of the thermal velocity and is very close to Ω for large values of V_{th}/V_d. The unstable modes tends to desappear for $V_{th}/V_d > 3$ which is not represented on the figure. Note that there are no more unstable roots for $k_y V_d > \omega_{UH}$ ($\omega_{UH}/\omega_{pe} = 1.005$) for very small temperature as it was found in section B. We also showed in that section that in the case $b \ll 1$, i.e, for very small thermal velocity, the unstable waves are almost purely imaginary. The frequency is several order of magnitude below the growth rate. In plasmas of interest of Hall thrusters, the thermal velocity is of the same order of magnitude as the drift velocity. So we can assume the thermal velocity as equal to half the drift velocity for all the following, so that the resolution of the dispersion relation would be simplified insofar the unstable modes are thick. It corresponds to temperature equal to $T = 5.7eV$. It is obvious that this is an arbitrary choice. However, the figure 3 shows that the main structure do not depend on the thermal velocity except for values we do not take account of.

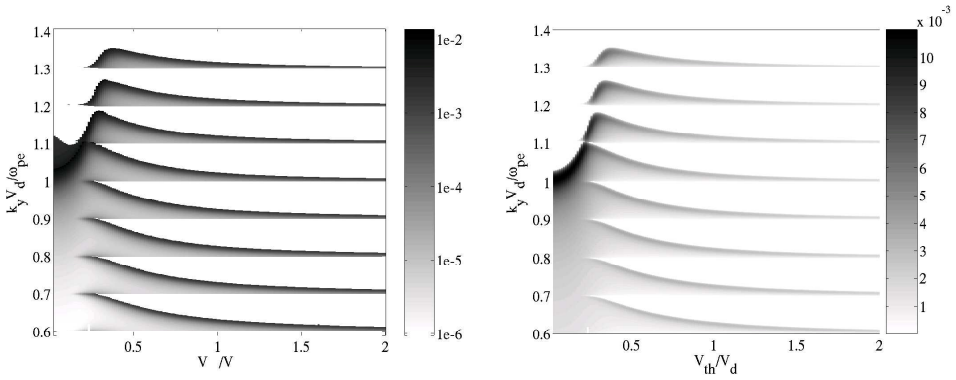

Figure 3. Frequency and growth rate as a function of V_{th}/V_d and of $k_y V_d$.

3. Influence of the density gradient

The analytic results of Sec.B tends to show that the gradient length must be very small to affect the property of the instability. In order to go further in the investigation of the effects of gradient density, Eq.(12) has been solved numerically. The results are summarized by Fig.4 which shows the growth rates as a function of $k_y V_d$ for three characteristic lengths of density gradient as defined in Sec.B. The lobes corresponding to typical gradient density in the thruster ($L_n \approx -1cm$) superimpose perfectly on the ones obtained without any gradient (solid line on the figure 4). The lobes in dashed line are the solution of the Eq.(12) for a strong gradient ($L_n = -0.05cm$). One can notice that the values of the growth rate are similar despite a weak decrease of the peaks. Nevertheless, the lobes are thicker than they are without any density gradient. It was predicted by the brief study on the dispersion relation (12): the additional term brought by the density gradient is significant only if the gradient length is much higher than the Larmor radius. In the Hall thrusters, the characteristic gradient length should be much smaller than $1mm$ so that the density gradient would affect the instability. This value is above the ones existing in the thruster, so we can consider that the instability is robust in relation to the gradient density.

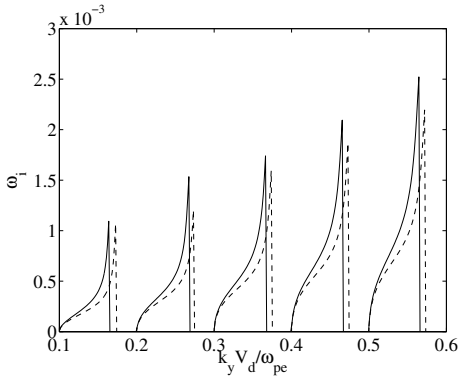

Figure 4. Effect of the gradient density.Solid line represents both the numerical solutions of 10 and 12 for $L_n = -1cm$. Dashed line is the growth rate for $L_n = -0.05cm$

The next section is devoted to a theoretical model for electron transport. It is based on the interaction between the instability studied above and the electrons in the configuration of electric and magnetic crossed

fields.

III. Electron transport

The problem of electron transport comes down to find a mechanism able to induce anomalous transport from an instability with a frequency very low what rules out a quasi linear diffusion.

A. Theoretical model

We consider the crossed field configuration of the thruster with the azimuthal instability introduced here as a monochromatic wave:

$$\vec{B} = B_0 \ \vec{e_z} \tag{15}$$

$$\vec{E_{stat}} = E_{stat} \ \vec{e_x} = -B_0 V_d \ \vec{e_x}; \quad V_d < 0 \tag{16}$$

$$\vec{E} = E_0 \ cos(k_y y - \omega t) \ \vec{e_y} \tag{17}$$

$\vec{E}$ represents the azimuthal drift instability determined by the study of the relation dispersion above. Its pulsation ranges from $1MHz$ to $50MHz$ and its wave number verifies $-k_y V_d \approx n\Omega_{ce}$ with n integer. We consider the electron-wave interaction on a time scale as the electron acts as though in a zero magnetic field[16]. So it requires $\omega \gg \Omega_{ce}$ which is not the case in the thruster. This assumption is possible insofar we introduce the Doppler shift induced by the drift motion of the electron. In the referential of the electron, drifting with the velocity $\vec{V_d}$, the electron motion comes down to a uniform cyclotron gyration perturbed by a fluctuating electric field. Setting $\eta = y - V_d t - Y$ where Y is the position of the guiding center of the electron ($\frac{dY}{dt} = 0$), the fluctuating electric field is written:

$$\vec{E} = E_0 \ cos(k_y \eta - (\omega - k_y V_d)t) \ \vec{e_y} \tag{18}$$

Then, for $n \gg 1$, we have $-k_y V_d \gg \Omega_{ce}$ and the wave frequency verifies: $\omega - k_y V_d \gg \Omega_{ce}$ The motion occurs in the plan (x, η) and the azimuthal component $\vec{e_y}$ of the motion equation is written:

$$\ddot{\eta} + \Omega^2 \eta = E_0 \ cos(k_y \eta - (\omega - k_y V_d)t) \tag{19}$$

The electron and the wave exchange most energy while in the resonance[16], i.e. when the η component of the electron velocity is close to the phase velocity of the wave:

$$V_\Phi = \frac{\omega - k_y V_d}{k_y} \approx -V_d = \dot{\eta} \tag{20}$$

where V_Φ is the phase velocity of the wave. The approximation $V_\Phi \approx V_d$ can be written as $k_y V_d \gg \omega$. It is obvious that the electron has to have enough energy so that its velocity component $\dot{\eta}$ could reach the phase velocity. Thus, we can say that the interaction electron-wave is efficient only if $V_\perp \geq -V_d$. In order to be exhaustive, we have to take into account the modulation due to the potential of the wave. This modulation corresponds to the nonlinear effect of trapping. This arises here because over a small part of an electron cyclotron orbit the effect of the magnetic field may be ignored. Then the condition on $V_\perp$ so that the electron could be in resonance with the wave becomes:

$$V_\perp \geq -V_d - \Delta v; \ \Delta v = \sqrt{\frac{2eE_0}{k_y m}} \tag{21}$$

where Δv is the trapping width.

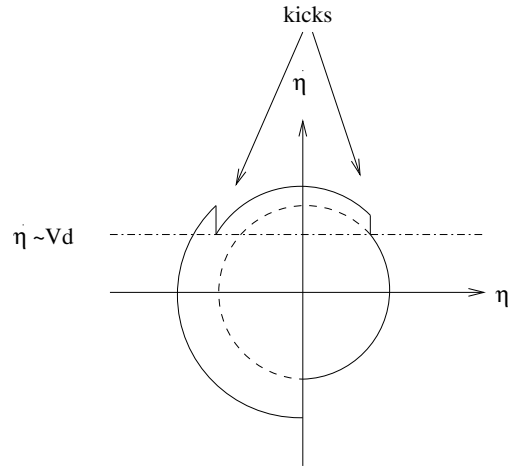

Figure 5. Schematic of electron orbit in the phase space $(\eta, \dot{\eta})$ for $V_\perp \geq -v_d - \Delta v$

Fig.5 shows the electron trajectory during a cyclotron gyration in the phase space when the condition (21) is verified. The main contribution of the wave to the motion takes place when the resonances occur. Such events ("kicks"), i.e when the condition (20) is verified, take place twice during a cyclotron period.

Except for the resonance, the electron trajectory remains close to a drifting cyclotron orbit. The two kicks received by the electron when passing through wave-particule resonance can be considered as wave-particle virtual collisions. According to the values of the amplitude of the wave E_0 and of the parameter $k_y V_d$, the electron orbit will be linearly perturbed or stochastic. The stochastic threshold is given by the following expression[16]:

$$\frac{E_0}{E_{stat}} > \Big(\frac{E_0}{E_{stat}}\Big)_{threshold} \approx \frac{1}{4}\Big(\frac{\Omega_{ce}}{k_y V_d}\Big)^{1/3} \tag{22}$$

For a fixed value of the parameter $k_y V_d$, i.e. for a given unstable mode, Eq.(22) gives the minimum ratio of the amplitude of the wave to the amplitude of the static field so that the electron trajectory would be stochastic. Below this threshold, the trajectory is slightly perturbed and oscillates around the drifting cyclotron orbit. Beyond this one, the electron trajectory becomes stochastic. For a population of electrons, it yields to a stochastic anisotropic diffusion in the phase space due to the asymmetry introduced by the electric static field. The next section is devoted to the numerical results associated to this theoretical model.

B. Results for unstable modes as $-k_y V_d \gg \Omega_{ce}$

The kinetic instability described above develops as $-k_y V_d \approx n\Omega_{ce}$. Therefore, it is obvious that the effect of each unstable mode cannot be studied with this theoretical model since it is available only for $-k_y V_d \gg \Omega_{ce}$. In particular, the first harmonic modes $n = 1, 2, 3...$ are too close to the cyclotron frequency so that one could dissociate the wave-particle interaction from the cyclotron motion. In such case one cannot consider any more that the wave-electron resonance, each time the condition (20) is true, occurs over a time short compared with the cyclotron period. So one cannot treated the interaction by assuming that the magnetic field is zero. Thus, the following results only concern the cases well descibed by the theory, e.g as $n \gg 1$. For the next figures, the values of the parameters are the same than in the section II: $\Omega_{ce} = 3GHz$, $\omega_{pe} = 30GHz$ and $V_d = 2\ 10^6 m.s^{-1}$. The unstable mode is chosen to verify the conditions $n \gg 1$ and $E_0/E_{stat} > (E_0/E_{stat})_{threshold}$: $E_0/E_{stat} = 0.5$ and $k_y V_d/\omega_{pe} = 1.017$(mode $n = 10$)

Fig.(6) shows clearly the scattering of the distribution function. The diffusion of the population of electrons occurs approximatively for $V_\perp$ higher than $V_\perp = 1.2\ 10^6 m.s^{-1}$ which is in a good agreement with

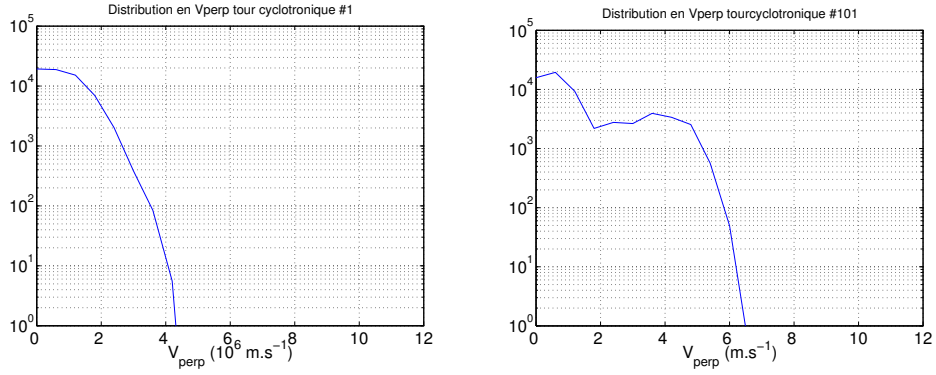

Figure 6. Electron distribution function versus $V_\perp$ at the origin (left) and after 100 cyclotron gyrations(right).The initial distribution is maxwellian with $T = 5.7$ eV

the condition (21) since with such parameters, $\Delta v = 0.89\ 10^6 m.s^{-1}$. The center of the distribution function remains unchanged as the electrons of low energy have a velocity not sufficient to reach the phase velocity of the wave (even when the trapping width is taken into account). For such electrons, there is no resonance and their interaction with the wave averaged on a cyclotron gyration is insignificant. The stochasticity of the electrons trajectories is clarified on the figure (7).

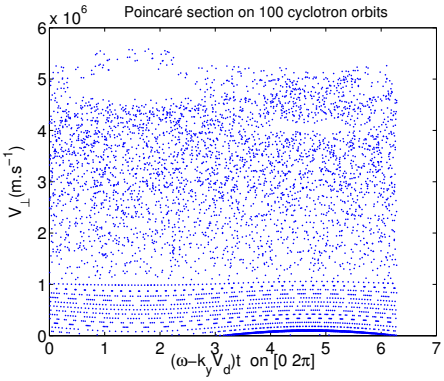

Figure 7. Poincaré Section. Each time the Larmor phase of the electron is equal to π, $V_\perp$ and time are mesured. It occurs one time per gyration and correponds to one dot. 50 electrons distributed homogeneously on $V_\perp \in [0, 4.10^6]$ are followed for 100 cyclotronic gyrations.

It represents the evolution of $V_\perp$ of 50 electrons as a function of $(\omega - k_y V_d)t$, which is approximatively proportionnal to the time, modulo 2π . The initial velocity of the electrons is distributed homogenously on $V_\perp \in [0; 4.10^6]$. The electrons trajectories are stochastic for $V_\perp \geq -v_d - \Delta v$. Below this value ($V_\perp \approx 1\ 10^6$) the trajectories are slightly perturbed: lines are formed by the successive dots. Above this value, the trajectories are not obvious any more, they are stochastic.

In Fig.(8) we have given the average on the distribution function of the electron velocity in the axial direction x as a function of time. It shows the existence of electron transport along the channel to the exhaust of the thruster with a rate close to the one we expect when one talk about anomalous transport.

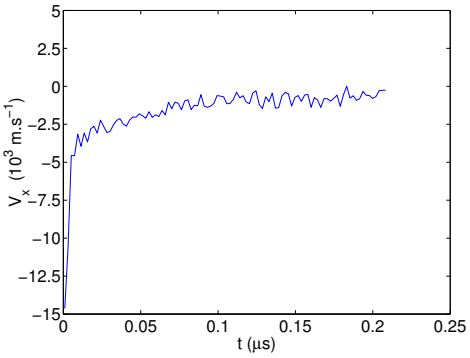

Figure 8. Average of the electron velocity on the distribution function in the axial direction x.

IV. Pic Simulations of the instability

Using a quasilinear formalism it is possible to compute an estimate of the transport across the magnetic field in the direction perpendicular to the drift velocity as in [1]. One obtains:

$$Vx \approx \sqrt(\pi/2)(m/T)(E_0/B)^2 \frac{V_d}{(2\sqrt(b))} \tag{23}$$

with $b = (k_y r_l)^2$, r_l is the Larmor radius

This crude estimate assumes that the distribution function is Maxwellian and that a stationary state has been reached. These assumptions have obviously no serious physical basis and have been made only to obtain an explicit expression of the average velocity. This expression shows that the average drift velocity across the magnetic field should be proportional to the square of the fluctuating field and also to the drift velocity. A series of 1D PIC simulations with geometry similar to the theoretical model (B constant perpendicular to the direction of simulation, E static parallel to the x direction yielding a drift velocity parallel to the direction of simulation) have been performed in order to check these dependencies. Preliminary results are shown in Fig.(9)

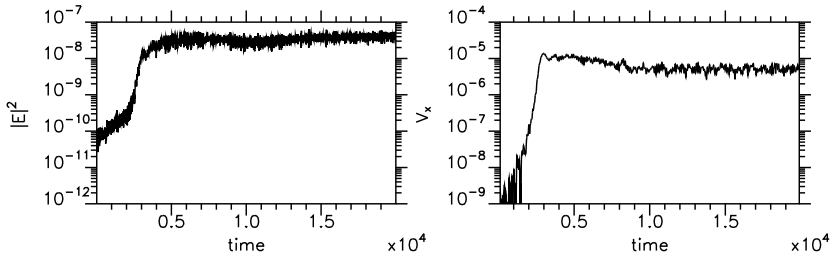

Figure 9. Correlation between the time evolution of the electrostatic energy and of the average velocity in the axial direction x. The electric unit is $e/(mc\omega_{pe})$ and v_x is v_x/c where c is the speed of light.

These simulations confirm the theoretical growth rate within 10% and also show the diffusion in velocity space around the drift velocity in agreement with the theory of section III. A strong correlation of the evolution of the electrostatic energy and the mean velocity across the magnetic field is visible in the Fig.(9). However due to the time evolution of the distribution function one can not expect to observe the exact proportionality predicted by the theory.

V. Conclusions

As a conclusion, we can say that the plasma configuration involving crossed electric and magnetic fields generate a high frequency drift instability based on the resonance between $k_y V_d$ and the cyclotron harmonics $n\Omega$ in frequency range $\Omega_{ci} \ll \omega \ll \Omega_{ce}$. It occurs for very short wavelength close or even below the electron gyroradius. The dispersion relation for these waves has been derived and numerically solved. We particularly paid attention on the drift modes whose robustness in relation to the temperature and the density gradient has been shown. The properties of the instability have been used to build a theoretical model. It describes well the wave-particle interaction for the very high wave numbers ($-k_y V_d \gg \Omega_{ce}$). For a sufficiently large amplitude of the wave, one can compared the wave-particle interaction to virtual collisions what generate a non isotrope diffusion in the axial direction due to the electric field. These theoretical results are in a good agreement with the results obtained by the PIC simulations. The strong correlation of the evolution of the electrostatic energy associated with the wave and the electronic transport is obvious. Work is underway to provide a better understanding of the saturation of the instability. The growth of the axial conductivity induced by the instability acts probably on the instability itself. The study of a self-consistent model belongs to the perspective to the presents works.

Acknowledgments

This work was performed in the framework of the GDR No 2232 CNRS/CNES/SNECMA/ONERA "Propulsions Plasma pour Systmes Spatiaux". Participation of A. Ducrocq was supported by the fellowship of CNES and SNECMA, France.

References

[1] J.C Adam, A. Heron and G. Laval,"Study of stationary thrusters using two-dimensional fully kinetic simultations", *Physics of Plasmas*, Vol. 11, No 1, 2004, pp. 295-305.

[2] E. Ahedo, J. M. Gallardo, and M. Martinez-Sanchez, *Physics of Plasmas*, Vol. 10, 2003, p. 3397.

[3] M. Keidar, I. D. Boyd, and I. I. Beilis, *Physics of Plasmas*, Vol. 8, 2001,p 5315.

[4]J. Bareilles, G. J. M. Hagelaar, L. Garrigues, C. Boniface, J. P. Boeuf, and N. Gascon, *Physics of Plasmas*, Vol. 11, 2004, p. 3035.

[5] J. M. Fife, Ph.D. thesis, Massachusetts Institute of Technologie, 1998

[6] J. J. Szabo, Ph.D. thesis, Massachusetts Institute of Technologie, 2001.

[7] O. Batishchev and M. Martinez-Sanchez, in *Proceedings of the* 28^{th} *International Electric Propulsion Conference*, IEPC 03-188, Toulouse, France, 2003.

[8] A. Smirnov,Y. Raitses and J. Fisch, *Physics of Plasmas*, Vol. 11, 2004, p. 4922.

[9] A. Lazurenko, V. Vial, M. Prioul and A. Bouchoule, *Physics of Plasmas*, Vol. 12, 2005, 013501.

[10] M.A. Capelli, N. Meezan, and N. Gascon "Transport physics in Hall thrusters",AIAA-2002-0485, *40th AIAA Aerospace Science Meeting and Exhibit*, Nevada, 2002.

[11] A. Bouchoule, M. Prioul, A. Lazurenko, V. Vial, J.C. Adam, A. Héron, and G. Laval, in *Proceedings of the 28th International Electric Propulsion Conference*, IEPC 03-218, Toulouse, France, 2003.

[12] N. A. Krall and P. C. Liewer, *Phys. Review A*, Vol. 4, 1971, p. 2094.

[13] N. A. Krall and D. L. Book, *Physics of Fluids*, Vol. 12, 1969, p. 347.

[14] B.D. Fried and S.D. Conte, *The Plasma Dispersion Functions*,Academic Press Inc., New York, 1961.

[15] A. Ducrocq, J. C. Adam, A.Héron and G. Laval, *Physics of Plasmas*(to be published)

[16] C.F.F. Karney, *Physics of Fluids*, Vol. 21, 1978, p. 1584; Vol. 22, 1979, p. 2188.